NJC

PAPER

View Article Online
View Journal | View Issue

Cite this: *New J. Chem.*, 2016, **40**, 10526

Crystal structure and physical properties of 1-methyl-3-(carboxymethyl)benzimidazolium betaine·$CuBr_2$ in crystal and water solution†

Łukasz Czekański,[a] Stanisław K. Hoffmann,*[b] Piotr Barczyński,[a] Anna Gąsowska,[a] Romualda Bregier-Jarzębowska,[a] Alina Zalewska,[a] Janina Goslar,[b] Małgorzata Ratajczak-Sitarz[a] and Andrzej Katrusiak[a]

Received (in Victoria, Australia) 11th October 2016,
Accepted 9th November 2016

DOI: 10.1039/c6nj03192g

www.rsc.org/njc

A new Cu(II) carboxylate coordinating compound [1-methyl-3-carboxymethyl benzimidazolium betaine]$_2CuBr_2$ was synthesized and crystallized. The crystal has the triclinic symmetry $P\bar{1}$, with unit cell dimensions a = 7.9693, b = 8.4129, c = 9.1302 Å, α = 68.058, β = 85.402 and γ = 71.258 deg. (Z = 1), and molecules stacked along the a-axis. Cu(II)-complexes are planar and four-coordinated with chromophore CuO_2Br_2, where two oxygen atoms belong to the carboxylate groups of two betaines acting as unidentate ligands. The compound was characterized by two-dimensional ^{1}H and ^{13}C NMR spectroscopy for the determination of the correlation between protons of a ligand molecule. NMR spectra confirm the coordination of Cu(II) ions and allow identification of H(2) proton as easily detached in basic conditions. FT-IR spectra confirm the unidentate coordination of the betaine carboxylate group. UV-Vis spectra show three bands in d–d-transition region. Energies of these transitions were used in the interpretation of the EPR results. From powder and single crystal EPR measurements the g-factors were determined as g_x = 2.072, g_y = 2.030, g_z = 2.241. A non-typical g-factor sequence is a consequence of the orbital mixing in the ground state of Cu(II) complex of D_{2h} symmetry. The g-factors were interpreted in terms of the Molecular Orbital (MO) theory which delivered the Cu(II) unpaired electron density delocalization onto the ligand molecules. A strong delocalization on betaine molecules *via* in-plane ground-state orbital was found and unexpectedly also *via* out-of plane orbital directed towards the non-coordinating oxygen of the betaine carboxylate group.

1. Introduction

Heterocyclic compounds, especially benzimidazole, triazole, pyridine,[1–3] and their derivatives are very often used as coordination agents.[4,5] Because of having a free electron pair on nitrogen atoms, those compounds can easily form complexes with transition metals and rare earth metals. Their excellent coordination capability opens possibilities of forming new functional materials and potential broad applications in chemistry and biology. Structures they form are very interesting because of their topology and architecture – forming MOF's (metal–organic frameworks) or POM's (poly-oxometalates). Moreover, they have potential applications in molecular recognition, absorption, fluorescence, catalysis, magnetism and as well as biological properties. An imidazole ring is a part of bioactive molecules (histamine, histidine, urocanic acid) and a number of drugs that stimulate the nervous system as well as being used in the treatment of leukemia (*e.g.*, cimetidine, tizanidine, tazoline).[6] Imidazoles attached to RNA affect folding of the molecules providing osmotic stress in hydration of the base pairs.[7] Beyond pharmaceutical interests, imidazole and its derivatives are one of the most important families in the field of heterocyclic chemistry and are of particular interest in agrochemical industries.[4,5,8–14] Imidazole derivatives have been developed as commercial fungicides and herbicides due to their antifungal and antimicrobial activities.[15,16] Naturally occurring di-(carboxyalkyl)-imidazole compounds are responsible for the taste, smell and color of food undergoing processes of frying or baking.[17]

A great importance is a conformational flexibility, which is responsible for *syn* and *anti* conformation of the ligand leading to divergent and convergent products with suitable metal ions.[1,18–20] Working-sheets about benzimidazole derivatives containing carboxylate groups coordinated to the different

[a] *Faculty of Chemistry, Adam Mickiewicz University in Poznań, Umultowska 89b, 61-614 Poznań, Poland*
[b] *Institute of Molecular Physics, Polish Academy of Sciences, Smoluchowskiego 17, 60-179 Poznań, Poland. E-mail: skh@ifmpan.poznan.pl*

† Electronic supplementary information (ESI) available: Atomic coordinates and equivalent isotropic displacement parameters (Table S1), bond lengths and angles (Table S2), torsional angles (Table S3), FT-IR absorption maxima (Table S4). CCDC 1480526. For ESI and crystallographic data in CIF or other electronic format see DOI: 10.1039/c6nj03192g

metals have been recently published.[9–14] Scientists are trying to investigate the relationship, biological activity and connections of heterocyclic complexes with Cu(II) with biological molecules such as peptides or DNA.[21–29] Liu and coworkers investigated the structure and DNA-condensing properties of tris(benzimidazolyl)amine–Cu(II) coordination units bridged by carboxylates, which can act as a new type of gene-delivery systems.[21]

The betaine derivative forms a large molecule with coordinating properties related to COO-group. Free betaine appears in a zwitterionic form $Me_3N^+CH_2COO^-$. Betaines are involved in the methylation reaction of biomolecules and are used by cells for the protection against osmotic stress. Metal–betaine interactions have been intensively studied in a series of coordination polymers where betaine molecules act as bridging units in dimeric and chain structures.[30–32] In most cases the betaine acts as a bidentate ligand although discrete molecules with betaine as unidentate ligand are known as well.[33] A characteristic feature of betaine is a larger O–C–O bond angle compared with common carboxylates resulting in better solubility.[33] Cu(II) ions are easily coordinated by betaine carboxylate group and halide anions Cl^- or Br^-. In binuclear Cu(II) complexes with bridging betaines the Cl and Br are located in apical positions.[33,34] In monomeric Cu(betaine)$_2$Cl$_2$ two chlorine atoms and two unidentate betaine form compressed tetrahedral $CuCl_2O_2$ units,[33] whereas when water molecule is involved, the square–pyramidal complexes are formed with two unidentate betaine and Cl or Br in a basal plane and a water molecule in an apical position.[30]

In this paper we report the synthesis and crystallization of a new coordination compound of Cu(II)Br$_2$ and *N*-alkylcarboxybenzimidazole as a ligand with monodentate carboxylate group of a betaine unit. Perfectly planar CuO_2Br_2 complexes were found in a crystal structure.

A triclinic crystal structure was determined by X-ray diffraction and correlated to the infrared vibrations. Measurements of powder and single crystal electron paramagnetic resonance (EPR) spectral parameters and their analysis by Molecular Orbital theory gave detailed electronic structure of the Cu(II) complex with delocalization parameters of unpaired electron density *via* the d-orbitals.

2. Experimental

2.1 Synthesis of materials

The final product was obtained in a four-step synthesis route using commercially available starting materials: 1-methylbenzimidazole (Sigma-Aldrich), ethyl bromoacetate (Sigma-Aldrich) and $CuBr_2$ (Merck).

1-Methyl-3-(ethoxycarbonylomethyl)benzimidazolium bromide – MBImAcOEt Br (1). To the flask, placed on a magnetic stirrer, MBIm ($n = 3.88 \times 10^{-3}$ mol) dissolved in anhydrous DMF ($V = 2$ cm^3) was added. The flask was flushed with argon. After this ethyl bromoacetate ($n = 4.656 \times 10^{-3}$ mol) was added drop wise. The reaction was carried out for 1.5 h, in 60 °C. After this solvent was evaporated on oil bath and the crude product was crystallized from acetone/MeOH. Yield 93%. Melting point = 156–158 °C.[35] The reaction was monitored by the thin layer chromatography-TLC (mobile phase: $CHCl_3$: MeOH = 3 : 1). $C_{12}H_{15}BrN_2O_2 \cdot 0.25H_2O$: calcd C 47.42, H 5.10, N 9.22; found C 47.34, H 5.40, N 9.26.

1-Methyl-3-(carboxymethyl)benzimidazolium bromide – MBImAcOH Br (2). To the compound (**1**) ($n = 3.88 \times 10^{-3}$ mol) 1.5 excess of 40% water solution of HBr ($n = 5.8 \times 10^{-3}$ mol) was added and the reaction was carried out for 10 h in reflux. After this time, the excess of water was evaporated. Precipitation was filtrated and crystallized forming iPrOH : MeOH (2 : 1). Yield 82.4%. Melting point = 234–235.5 °C. $C_{10}H_{11}BrN_2O_2$: calcd C 44.3, H 4.06, N 10.35%; found C 44.4, H 4.25, N 10.34%. Selected IR data (nujol/fluorolube, cm^{-1}): 1737 (COOH); 1572, 1487, 1465 (νC=C); 1451, 1430 (δCH); 1396 (ν_sCOO); 986, 89, 884, 864, 830, 772 (γCH); 629, 601, 576, 526 (skeletal vibrations).

1-Methyl-3-(carboxymethyl)benzimidazolium betaine – MBImAcO (3). To the flask, placed on a magnetic stirrer, (**2**) ($n = 9.2 \times 10^{-3}$ mol) dissolved in 20 ml of methylene chloride was added (hydrobromide did not dissolve completely even after heating). Septa was applied to the neck of the flask and flushed with argon, Et_3N ($n = 9.2 \times 10^{-3}$ mol) was added. Then the balloon was filled with Ar and allowed the contents of the flask stay in the argon atmosphere with stirring on a magnetic stirrer for 12 hours at room temperature. The precipitated solid was filtered off, washed with $CHCl_3$ and crystallized from EtOH to give 3-(carboxymethyl)-1-methyl-benzimidazolium betaine as a fine crystalline solid. The reaction yield is 88.6%. Melting point = 225–228 °C.[36] $C_{10}H_{10}N_2O_2 \cdot 0.5H_2O$: calcd C 60.23, N 14.05, H 5.52; found C 60.45, N 14.01, H 5.73. Selected IR data (nujol/fluorolube, cm^{-1}): 3466, 3396 (νOH); 3137, 3059 (νCH); 1616 (ν_{as}COO); 1569, 1488, 1466 (νC=C); 1414 (δCH); 1377 (ν_sCOO); 986, 902, 872, 811, 780, 760 (γCH); 659, 591, 525 (skeletal vibrations).

The synthesis of the compounds (**1–3**) is presented in Scheme 1.

1-Methyl-3-carboxymethyl benzimidazolium betaine with $CuBr_2$-[Cu(MBImAcO)$_2$Br$_2$] (4). The resulting complex was prepared by mixing the excess of 1-methyl-3-carboxymethyl benzimidazolium betaine ($n = 1.051525 \times 10^{-3}$ mol) with $CuBr_2$ ($n = 0.262881 \times 10^{-3}$ mol) in methanol at room temperature, for 15 min. The precipitate was crystallized from water to give green crystals (Scheme 2). Melting point = 180–183 °C. $C_{20}H_{20}Br_2CuN_4O_4$: calcd C 39.79, H 3.34, N 9.28%; found C 39.85, H 3.44, N 9.23%. Selected IR data (KBr, cm^{-1}): 3148, 3030 (νCH); 1626 (ν_{as}COO); 1575, 1487, 1468 (νC=C); 1437, 1423 (δCH); 1375 (ν_sCOO); 981, 923, 886, 798, 772, 757, 750 (γCH); 668, 614, 572, 530 (skeletal vibrations). ESI-MS (solvent MeOH, mass range: 100–1000): ES-picks: 221–227 [m/z] are from $[CuBr_2]^-$ isotopes and picks: 300–308 are from $[CuBr_3]^-$ isotopes; ES+: ligand mass = 190 [g mol^{-1}] – L; 191[m/z] – protonated ligand – $[L + H]^+$, 253[m/z] – ligand + Cu – $[L + Cu]^+$, 381[m/z] – $[2 \times L + H]^+$, 443[m/z] – $[2 \times L + Cu]^+$, 524[m/z] – $[2 \times L + Cu + Br]^+$, 571[m/z] – $[3 \times L + H]^+$.

2.2 Physical measurements

Elemental analysis for the percentage of C, N and H in a sample was performed on a Vario EL III Elementar German company.

FT-IR spectra were taken on a Bruker IFS 66 v/S. Samples of solid compounds were prepared as suspensions in Nujol and

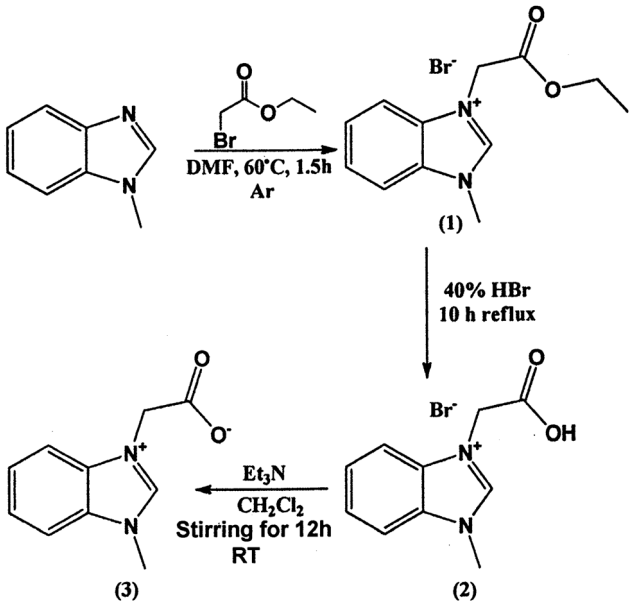

Scheme 1 Synthesis of the ligand 1-methyl-3-carboxymethyl benzimidazolium betaine.

Fluorolube, and KBr film. The spectra were recorded in the range of mid-infrared 4000–400 cm^{-1} with resolution 2 cm^{-1}. Each FT-IR spectrum was measured by acquisition of 64 scans.

UV-Vis spectra were taken on a UV/Vis Thermo Fisher Scientific Evolution 300 Spectrophotometer. The samples were prepared in H_2O for the same ligand and metal concentration as in samples for potentiometric titrations using a Plastibrand PMMA cell with 1 cm path length.

^1H and ^{13}C NMR was performed on a Varian 400 MHz and 2D ^1H and ^{13}C NMR was performed on a Bruker Avance 600 MHz. The 2D ^1H–^1H (COSY), ^1H–^{13}C (HETCOR) and HMBC (Heteronuclear Multiple-Bond Connectivity) spectra were obtained with the standard Bruker software.

The $Cu(MBImAcO)_2Br_2$ crystals selected for single-crystal X-ray diffraction measurements were grown from water as green parallelepipeds. They were stable under normal conditions and the X-ray diffraction measurements were carried out on a Eos X-Calibur diffractometer using MoKα radiation at room temperature: ω-scan data collection with $\Delta\omega = 1^\circ$ frames and 40 s exposures was applied. Data reduction was performed with the CrysAlisPro and CrysAlisRed programs.[37] The absorption of crystal was corrected analytically. The max. and min. transmissions were 0.6205 and 0.3033, respectively. The structure was solved by direct methods using SHELXS-97 and refined with full-matrix least-squares on reflections intensities (F^2) with SHELXL-97.[38] All H-atoms were located from the molecular geometry (C–H 0.93–0.97 Å) and their U_{iso}'s were assigned equal to $1.2U_{eq}$ of their carriers, and $U_{iso} = 1.5U_{eq}$ for the methyl group.

Powder and single crystal EPR spectra were recorded at room temperature and at 77 K using Radiopan SE/X-2547 spectrometer working at X-band with 100 kHz modulation. The spectra were simulated using Bruker SimFonia routine. Angular dependence of the single crystal EPR line was measured in three planes of an orthogonal reference frame 1, 2, 3 related to the crystal plate. Axis 1 is parallel to the [001] direction being the elongation direction of the crystal plane, and axis 3 is perpendicular to the largest crystal face$(1\bar{1}\bar{1})$.

3. Results and discussion

The 1-methyl-3-carboxymethyl benzimidazolium betaine ligand (**3**) and its complex with $CuBr_2$ (**4**) were synthesized. They were characterized by various spectroscopic methods to find correlation between crystal structure and observed chemical and physical properties.

3.1 Ligand and Cu-complex characterization by ^{13}C and ^1H NMR

The benzimidazole betaine ligand (**3**) and Cu-complex (**4**) synthesizes as shown in Schemes 1 and 2, were characterized by 2D NMR spectroscopy in order to assign the exact position of the protons and carbons derived from a benzimidazole ring and possible correlation between atoms through the scalar J-coupling. NMR spectra of benzimidazolium betaine ligand were made in D_2O. ^1H and ^{13}C NMR chemical shifts assignments from HMBC experiment are listed in Scheme 3 and 2D spectrum is shown in Fig. 1. The horizontal axis corresponds to ^1H spectrum and the vertical axis to the ^{13}C spectrum. Proton H(2) peak is not shown in the spectrum, because the acidic H(2) proton was exchanged on the deuterium. Trace amounts of H(2) are visible at a high zoom. The H(12) signal is coupled to the peaks representing C(2) and C(5) through three bonds. As expected, the H(10) signal is coupled to the peaks C(4), C(2) through three bonds and C(11)OO through two bonds. Signals: H(6) is coupled to the peaks C(8) and C(4); the H(9) is coupled to the peaks C(7) and C(5) through the three bonds.

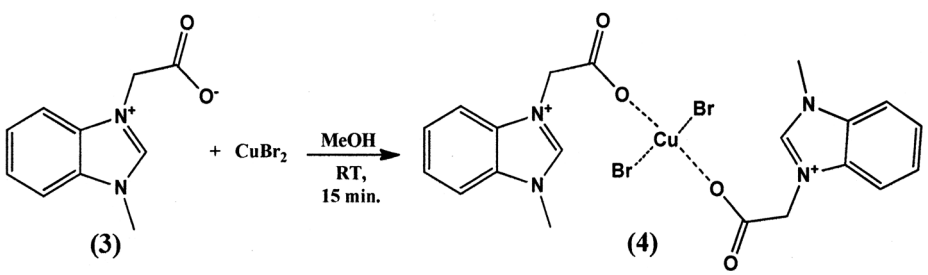

Scheme 2 Synthesis of complex of 1-methyl-3-carboxymethyl benzimidazolium betaine with $CuBr_2$.

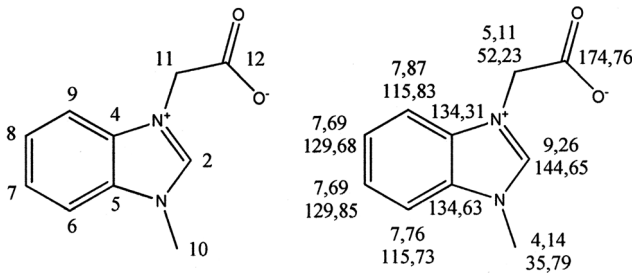

Scheme 3 Numbering of atoms in ligand molecule and chemical shift for ^{1}H (upper number) and ^{13}C (lower number).

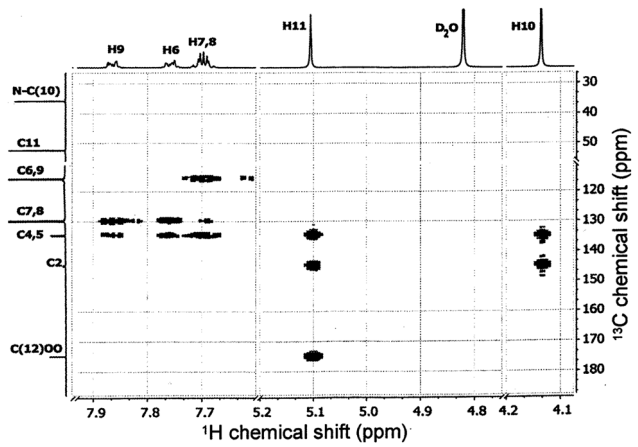

Fig. 1 2D NMR (HMBC) spectra of benzimidazolium betaine ligand (**3**) in D_2O.

^{1}H and ^{13}C NMR spectra of benzimidazolium betaine ligand (**3**) and the complex (**4**) (which was made by mixing betaine (**3**) with $CuBr_2$, in the ration 100 : 1), were made in D_2O and are compared in Fig. 2 and 3. In ^{13}C NMR spectrum of complex (**4**), carboxylate carbon atom C(12) appears as an extended, small peak, which demonstrates the coordination of the copper atom through an oxygen atom bonded directly to a carboxylate carbon atom. Moreover, the peak from carbon atom C(11) almost disappears. At high magnification, it appears to be an expanded signal. It also suggests that there is a coordination of copper atom through carboxylate group which is directly attached to the carbon C(11). All signals of carbons C(4)–C(9) in the benzene ring are distinguishable, because of unsymmetrical substitution of imidazole ring.

The position C(2) has acidic properties, making it easy to detach the H(2) proton at basic conditions. Due to the fact that ^{13}C NMR spectrum of the betaine (**3**) was made in D_2O, there is an exchange of a proton H(2) by deuterium atom, which gives three signals in the spectrum. These signals are the result of coupling of the carbon atom C(2) with deuterium atom, while in the ^{13}C NMR spectrum of the complex (**4**), there are four signals: singlet and triplet. The singlet derived from coupling of C(2) with proton H(2) – incompletely deuterated C(2) position of the ligand. The triplet signal is the result of the coupling of carbon atom C(2) with deuterium atom from the solvent. A comparison of the ^{13}C chemical shifts of benzimidazolium betaine (**3**) and complex (**4**) shows that only the shifts of C(11) and C(12)OO of betaine are affected by copper(II) coordination through the carboxylate group. The chemical shifts are: from 174.76 ppm to 173.94 ppm for C(12)OO and from 52.24 ppm to 54.76 ppm for C(11).

^{1}H NMR spectrum of betaine ligand (**3**) (Fig. 3) was made in D_2O. Therefore, there has been almost full exchange of proton H(2) into the deuterium atom. After enlarging, traces of proton H(2) are visible. Whereas in the spectrum of the complex (**4**) we can observe a signal from H(2), which has not been completely exchanged for deuterium atom. From the curve of integration,

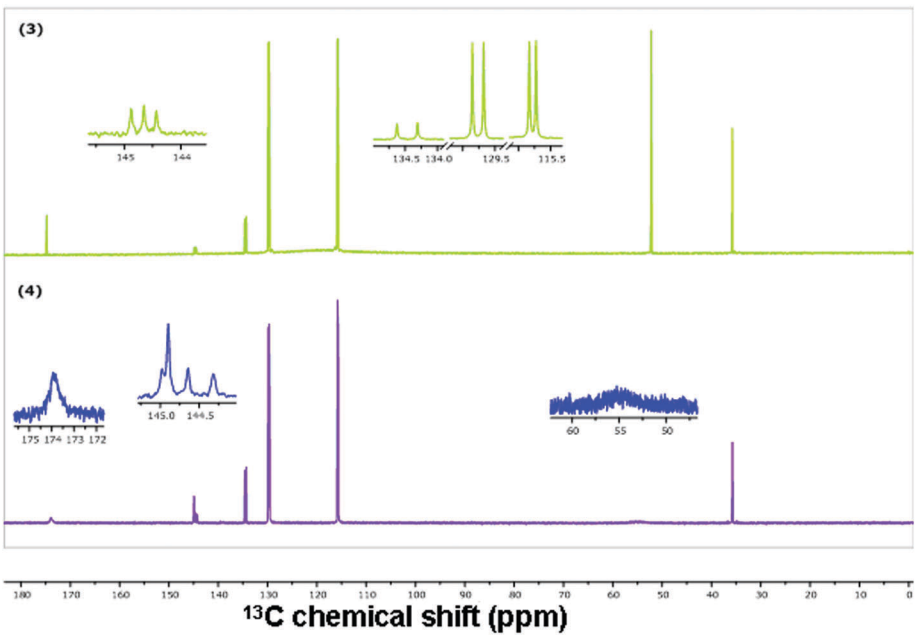

Fig. 2 ^{13}C NMR spectra of benzimidazolium betaine ligand (**3**) and of Cu(II) complex (**4**) in D_2O.

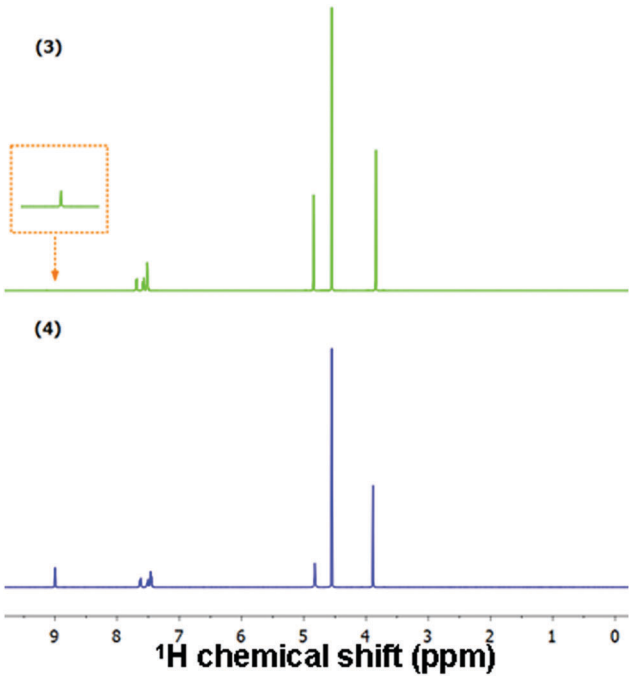

Fig. 3 ^{1}H NMR, spectra of benzimidazolium betaine ligand (**3**) and of the Cu-complex (**4**) in D_2O.

we can conclude that about 20% of H(2) has been exchanged. Comparing the signal positions of the ligand and Cu-complex we cannot see any significant differences.

3.2 Crystal structure

The crystal data and details of the data collection and structure refinement of [1-methyl-3-carboxymethyl benzimidazolium betaine]$_2$CuBr$_2$ are given in Table 1, and the atomic coordinates are listed in ESI† (Table S1). CCDC 1480526. Structural drawings were prepared using ORTEPII and XP programs.[39,40]

The complex (**4**) is formed by the Cu(II) cation coordinated by two Br anions and two zwitterionic MBImAcO molecules. Each MBImAcO molecule forms a unidentate type of coordination bond through its carboxylate oxygen O(2) to the Cu(II) cation (Fig. 4).

The Cu(II) cation is located at the inversion centre. Consequently, the benzimidazole rings of the ligands are mutually parallel as required by the crystal symmetry as it is visible in autostereographic projection of Fig. 5.[41] Thus, also the all carboxylate groups in the crystal are mutually parallel. The carboxylate group is twisted by 77.5(2)° from the plane of the benzimidazole ring. There is one [Cu(MBImAcO)$_2$Br$_2$] complex molecule per the unit cell and half of the complex is symmetry independent. The molecules form chains along the crystal *a*-axis with stacked benzimidazole rings.

CuO_2Br_2-complex is planar with Cu(1)–O(2) distance equal to 1.9293 Å and Cu(1)–Br(1) bond 2.4125 Å. The second oxygen atom of the betaine is at longer distance Cu(1)–O(1) = 2.9492 Å and does not disturb the square-planar geometry of CuO_2Br_2-complex. The perfect planarity of CuO_2Br_2-complex is an effect of a weak coupling of Br-atom to the lattice allowing the electrostatic forces to form the linear Br–Cu–Br bond. However, a planar structure is not an intrinsic property of four coordinated

Table 1 Crystal data and structure refinement

Empirical formula	$C_{20}H_{20}N_4O_4Br_2Cu$
Formula weight	603.76
Temperature (K)	293(2)
Wavelength	0.71073 Å
Crystal system, space group	Triclinic, $P\bar{1}$,
Unit cell dimensions	a = 7.9693(5) Å
	b = 8.4129(5) Å
	c = 9.1302(5) Å
	α = 68.058(5)
	β = 85.402(5)
	γ = 71.258(6)
Volume	537.13(5) Å^3
Z	1
Calculated density	1.867 g cm^{-3}
Absorption coefficient	4.772 mm^{-1}
F(000)	299
Crystal size	0.25 × 0.20 × 0.10 mm
θ range for data collection	2.41–29.12°
Limiting indices	$-9 \le h \le 10$, $-11 \le k \le 8$, $-12 \le l \le 12$
Reflections collected/unique	4820/2515 R_{int} = 0.0212
Completeness to θ = 29.12	87.4%
Refinement method	Full-matrix least-squares on F^2
Data/restraints/parameters	2515/0/142
Goodness-of-fit on F^2	1.008
Final R indices [$I > 2\sigma(I)$]	R_1 = 0.0290, wR_2 = 0.0681
R indices (all data)	R_1 = 0.0398, wR_2 = 0.0722
Largest diff. peak and hole	0.405 and −0.513 e Å^{-3}

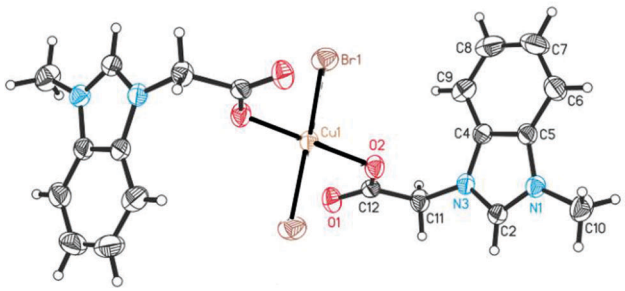

Fig. 4 Perspective ORTEP drawing of complex Cu(MBImAcO)$_2$Br$_2$ with atom numbering. The thermal ellipsoids are shown at 50% level.

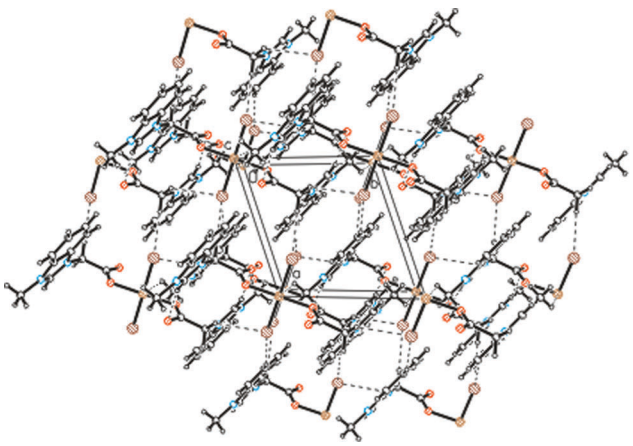

Fig. 5 Autostereographic projection[41] of the molecular packing in crystal structure of Cu(MBImAcO)$_2$Br$_2$ viewed along [001]. The shortest H···Br contacts are indicated by the dashed lines.

Cu-complexes with identical ligand atoms. A free CuX_4 tetrahedron has distorted geometry being a result of a balance between crystal field stabilization favoring square-planar geometry and Br–Br electrostatic repulsion favoring tetrahedral geometry. This balance is reached for Br–Cu–Br angle of about 120°. Hydrogen bonds tend to remove the charge from bromine atoms reducing electrostatic repulsion and thus enhancing a tendency to square-planar coordination. Crystal packing effect resulting from alignment of large organic molecules and hydrogen bonds can dominate the intrinsic effect leading to the planar geometry even for CuX_4 complexes.

Two of the shortest intermolecular contacts with respect to the van der Waals radii have the forms of a weak CH···Br hydrogen bonds: Br(1)···H(112)–C(11) (symmetry code: $1-x$, $2-y$, $2-z$) and Br(1)···H(111)–C(11) (symmetry code: $x, y-1, z$). Their H···Br distances of 2.720 and 2.988 Å are by 0.31 and 0.04 Å, respectively, shorter than the sum of the van der Waals radii of H and Br (1.2 and 1.83 Å according to ref. 42). The next shortest contacts between the complex aggregates are all longer than the sums of van der Waals radii. The bond lengths and bond angles are presented in Tables S2 and S3 of the ESI.†

3.3 Vibrations of benzimidazole betaine (3) and Cu-complex (4) studied by FT-IR

FT-IR spectra of free ligand (**3**) and Cu(II)-complex (**4**) are compared in Fig. 6. Band assignment is given in the Experimental section and compared for benzimidazolium hydrobromide (**2**), benzimidazolium betaine ligand (**3**) and Cu(II)-complex (**4**) in Table S4 at ESI.†

Broad band with resolved peaks at 3466 cm^{-1} and 3396 cm^{-1} in ligand spectrum can be assigned as stretching vibrations of OH-groups indicating the existence of a single water molecule attached to the betaine ligand. This band does not exist in the Cu(II) complex (**4**) confirming that the final green crystal does not contain water molecules. The antisymmetric O–C–O stretching mode 1616 cm^{-1} for ligand (**3**) is shifted to 1626 cm^{-1} indicating the coordination of Cu(II) ion by the carboxylate group. The coordination with the bromine atom is not detectable in the presented spectrum. Cu–Br antisymmetric and symmetric stretching vibrations are expected in 240–250 cm^{-1} and 200–210 cm^{-1} region, respectively,[43] which are out of range of our measured spectrum.

A coordination type can be established by a comparison of the symmetric (ν_s-COO) and antisymmetric (ν_{as}-COO) stretching modes frequencies. It is known that the frequency difference $\Delta = \nu_{as} - \nu_s$ between these modes is in the following order: Δ(unidentate) > Δ(ionic) ~ Δ(bridge) > Δ(bidentate).[44–46] If the difference Δ is lower than the 203 cm^{-1} (observed value for sodium acrylate), then we are dealing with the type of bidentate coordination. In contrast, when this value is greater than 203 cm^{-1}, this shows unidentate coordination. Frequencies ν_s(COO) and ν_{as}(COO) of the symmetric and antisymmetric O–C–O stretching modes of the coordinated formate ion in (**4**) are assigned at 1375 and 1626 cm^{-1}, respectively. Value Δ = 251 cm^{-1} suggests a unidentate coordination mode between Cu ion and carboxylate group of a betaine ligand.

3.4 Orbital d–d transitions of Cu-complex (4) in UV-Vis spectrum

UV-Vis spectrum of the complex (**4**) is shown in Fig. 7 with an inset presenting enhanced spectrum in the Cu(II) d–d transition region. The d–d region can be decomposed on the three bands as shown by the dashed lines and can be assigned as transitions from the ground state $|x^2-y^2\rangle$ of symmetry A_g to excited orbitals in D_{2h} complex symmetry as: $|xy\rangle$ (B_{1g}-symmetry) at 12 594 cm^{-1}, $|xy\rangle$ (B_{2g}-symmetry) and $|yz\rangle$ (B_{3g}-symmetry) at 15 198 cm^{-1}, and $|z^2\rangle$ (A_g-symmetry) at 17 065 cm^{-1}. It is a typical sequence of orbital energies for the planar or strongly elongated octahedral Cu(II) complexes.

The spectrum at UV-region can be decomposed on four bands located at 253 nm, 277 nm, 339 nm and 397 nm resulting from intramolecular transitions.

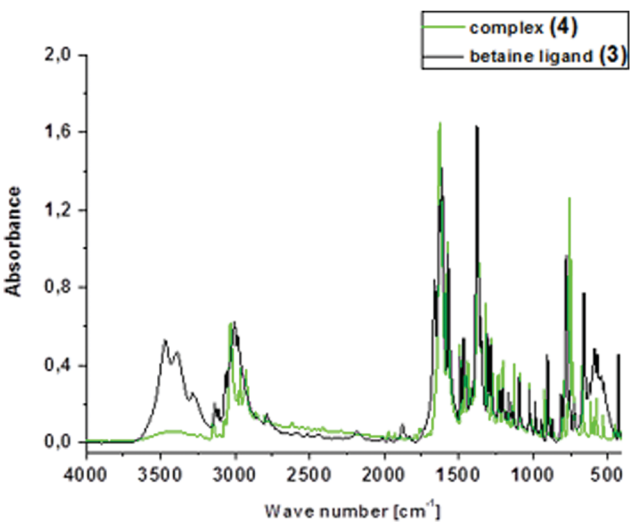

Fig. 6 FT-IR spectra of benzimidazolium betaine (**3**) and the Cu-complex (**4**).

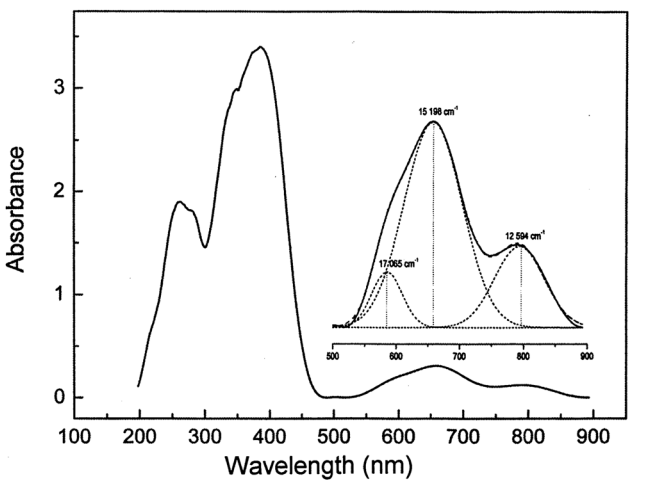

Fig. 7 UV-Vis spectrum of Cu(II)-complex (**4**). The inset shows region of d–d transitions decomposed on three bands (short dashed lines) located at 586, 658 and 794 nm, corresponding energies in cm^{-1} are shown, respectively. The sum of the bands (dashed line) is perfectly superimposed on the experimental spectrum.

3.5 Electronic structure of Cu-complex (4) crystal from EPR spectroscopy

In the case of triclinic crystals of magnetically condensed paramagnets, EPR allows a determination of the local magnetic properties of individual Cu(II) complex. It is possible since for a single complex in the crystal unit cell ($Z = 1$) a single resonance line is observed with parameters not averaged by exchange interaction between differently oriented (magnetically nonequivalent) complexes. Such a situation appears in $Cu(MBImAcO)_2Br_2$ crystal where a single nearly Lorentzian line is observed in all crystal orientations. Lorentzian lineshape suggests exchange coupling between Cu(II) ions. This coupling is rather weak but strong enough for smearing out of any expected hyperfine structure. One can expect maximal hyperfine splitting order of 20 mT from ^{63}Cu nuclei ($I = 3/2$) and 5 mT from $^{79,81}Br$ nuclei ($I = 3/2$).[47] This allows evaluation of exchange coupling as larger than 0.1 cm^{-1}. Thus, only the g-factor is an available EPR parameter since the linewidth varies only in the narrow range around 0.8 mT at room temperature and around 1.5 mT at 77 K.

EPR spectrum was recorded for powder samples and for single crystals. Powder spectrum recorded at room temperature and at liquid nitrogen temperature is presented in Fig. 8. The spectral parameters obtained from computer simulations of the powder spectra (dashed lines) are collected in Table 2. This is a typical spectrum described by non-axial $\boldsymbol{g}$-tensor. The shift of the low-field line, corresponding to the g-factor along the main complex symmetry axis (z-axis) and line broadening on cooling are non-typical behavior due to exchange and dipolar coupling competition.

More precise information on the $\boldsymbol{g}$-tensor and its orientation in the crystal one can obtain from the analysis of angular dependence of the resonance line position. Such measurements were performed by crystal rotation around three orthogonal axis of the reference frame related to the largest crystal plane($1\bar{1}\bar{1}$) as it is shown in the inset of Fig. 9. The $\boldsymbol{g}^2$-tensor components were calculated (see Table 2) and the tensor diagonalization gave the principal value and principal axes direction cosines (see Table 2). Principal values are in good agreement with the powder data. Principal $\boldsymbol{g}^2$-tensor directions show that the main symmetry axis of the CuO_2Br_2 complex (normal to the coordination plane) well coincides with local crystal z-axis (compare the results in Table 2) from EPR measurements. The Br^--ligand is a source of relatively weak crystal field (only I^- ion gives weaker) as shown by its localization in the spectrochemical series, and its contribution to crystal field at Cu(II) site is smaller than that from oxygen atom. Thus, the g-factor along O–Cu–O direction is expected to be the lowest giving g_x-value, whereas along Br–Cu–Br (y-axis) the medium value g-factor appears. Orbital mixing, discussed below, produces reversing the g_x and g_y values. The local crystal field axes x, y, z lie close to the planes of the reference frame as marked in Fig. 9 and the complex localization with local axes is shown in Fig. 10.

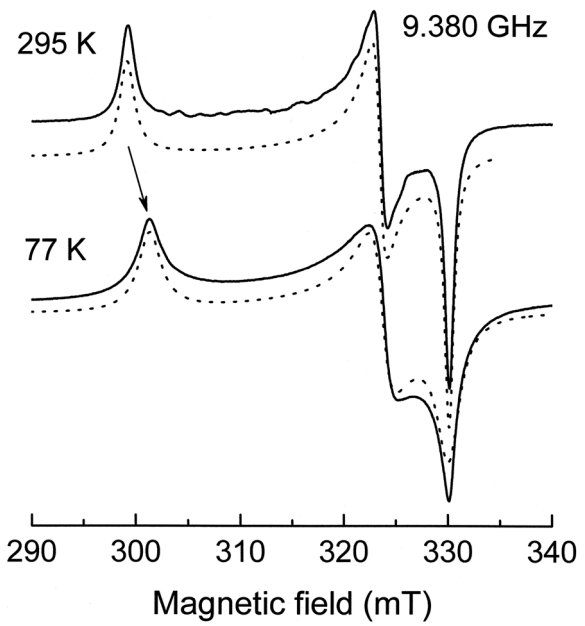

Fig. 8 Powder EPR spectrum of Cu(II) in $Cu(MBImAcO)_2Br_2$ recorded at room and liquid nitrogen temperature at frequency 9.380 GHz. Dashed lines are the simulated spectra with parameters collected in Table 2.

The minimal g-factor is lower than 2.04. It cannot result from the d-orbital splitting but it is an effect of the orbital mixing in the orbital ground state. Local geometrical and crystal field symmetry of the CuO_2Br_2 complex is D_{2h}. In this relatively low symmetry the orbitals having the same symmetry can be mixed. In D_{2h} the orbitals $|x^2 - y^2\rangle$ and $|z^2\rangle$ have A_g-symmetry and are mixed in the ground state leading to the anti-bonding molecular orbitals

$$\Psi(A_g) = \alpha(ad_{x^2-y^2} + bd_{z^2}) - \alpha' L_1$$

$$\Psi(A_g') = \alpha_1(ad_{z^2} - bd_{x^2-y^2}) - \alpha_1' L_2$$

$$\Psi(B_{1g}) = \beta d_{xy} - \beta' L_3$$

$$\Psi(B_{2g}) = \gamma_1 d_{xz} - \gamma_1{}^1 L_4$$

$$\Psi(B_{3g}) = \gamma_2 d_{yz} - \gamma_2' L_5 \quad (1)$$

where L_i are a linear combination of ligand orbitals s and p of appropriate symmetry and the mixing coefficients fulfill normalization condition $a^2 + b^2 = 1$.

For the A_g ground state symmetry the principal $\boldsymbol{g}$-tensor components are:[48]

$$g_z = 2.0023 - 8\alpha^2\beta^2 a^2 \frac{\lambda}{E_{xy}}$$

$$g_y = 2.0023 - 2\alpha^2\gamma_1{}^2\left(a - \sqrt{3}b\right)^2 \frac{\lambda}{E_{xz}} \quad (2)$$

$$g_x = 2.0023 - 2\alpha^2\gamma_2{}^2\left(a + \sqrt{3}b\right)^2 \frac{\lambda}{E_{yz}}$$

where λ = 829 cm^{-1} is spin–orbit coupling constant of Cu(II) and E_{ij} are orbital splittings.

The first, but mostly not obvious consequence of the mixing, hidden in eqn (2), is reversing the g-factors sequence with $g_x > g_y$. This appears even for a very small mixing effect.[48]

Table 2 Powder and single crystal EPR parameters

From powder spectrum simulations (with Lorentzian lineshape)			
Room temperature 295 K		Liquid nitrogen temperature 77 K	
$g_x = 2.072$	$\Delta B_{pp}(x) = 0.06$ mT	$g_x = 2.072$	$\Delta B_{pp}(x) = 1.5$ mT
$g_y = 2.030$	$\Delta B_{pp}(y) = 0.09$ mT	$g_y = 2.030$	$\Delta B_{pp}(y) = 1.5$ mT
$g_z = 2.240$	$\Delta B_{pp}(z) = 1.0$ 0 mT	$g_z = 2.234$	$\Delta B_{pp}(z) = 1.5$ mT

From single crystal rotational data at 295 K in 1, 2, 3 orthogonal reference frame

g^2-Tensor

$$g^2 = \begin{pmatrix} 4.49119 & -0.34719 & -0.27554 \\ -0.34719 & 4.52459 & +0.17086 \\ -0.27554 & +0.17086 & 4.431295 \end{pmatrix}$$

Principal value and directions

$$\begin{matrix} g_x = 2.074 \\ g_y = 2.030 \\ g_z = 2.241 \end{matrix} \begin{pmatrix} 0.022876 & 0.629145 & -0.77695 \\ -0.7684 & -0.48648 & -0.41584 \\ 0.6396 & -0.60645 & -0.47234 \end{pmatrix} \begin{matrix} x\text{-axis} \\ y\text{-axis} \\ z\text{-axis} \end{matrix}$$

The direction cosines of the normal to the CuO_2Br_2 coordination plane are: (0.6422, −0.5901, −0.4892).

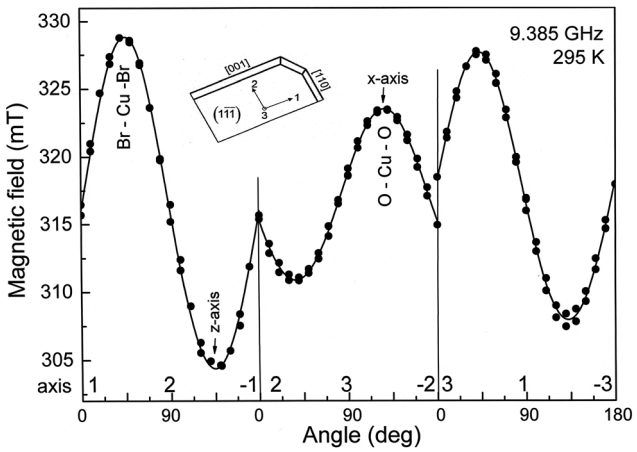

Fig. 9 Angular dependence of the resonance field in three planes of 1, 2, 3 orthogonal frame (see inset). Solid lines are theoretical plots with principal $\boldsymbol{g}$-tensor values and direction cosines given in Table 2. The z-axis and x-axis (close to the Cu–Br bonds) marked in the figure do not lie in the 12 and 23 planes but are close to the indicated directions (see corresponding principal direction cosines in Table 2).

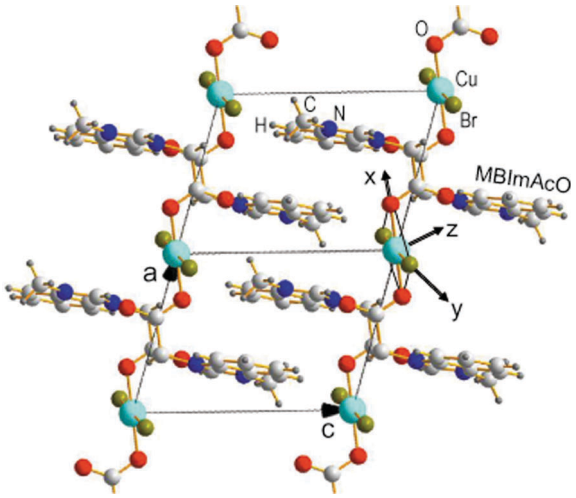

Fig. 10 Crystal structure view in the crystal rotation around the c-axis with Cu(II) complex localized in the unit cell corner with marked local crystal field axes x, y, z. The picture visualizes a stacked-type crystal packing with chain of $Cu(II)O_2Br_2$ complexes along the crystal a-axis.

From the analysis of eqn (1) using orbital energies from UV-Vis spectrum one can calculate molecular orbitals coefficients a, α, β, γ_1 and γ_2. These coefficients characterize electronic structure of the studied paramagnetic center, *i.e.* a degree of unpaired electron spin density localization onto central ion and delocalization *via* coordination bands. The coefficients cannot be exactly calculated from the three eqn (2) and the normalization condition. Thus, we propose approximate approach for the coefficient evaluation, with sufficiently good accuracy, taking into account that squared MO-coefficient cannot be lower than 0.5 (unpaired electron cannot be strongly delocalized onto ligands).

Mixing coefficient a can be evaluated from g_y value plotting α^2 *vs.* a using eqn (2). Since $\alpha^2 > 0.5$ thus from the plot $a = 0.964$–0.988. It is a relatively small orbital mixing in the ground state. From the equations for g_x and g_y the γ-values can be evaluated by plotting the ratio γ_1/γ_2 *vs.* a from the equation

$$\frac{\gamma_1}{\gamma_2} = \sqrt{\frac{\Delta g_y}{\Delta g_x}} \frac{a + \sqrt{3}b}{a - \sqrt{3}b} \qquad (3)$$

where $\Delta g_i = g_i - 2.0023$. From such the plot we concluded that ${\gamma_1}^2$ and ${\gamma_2}^2 = 0.5$–0.6, *i.e.* no delocalization *via* d_{xz}-orbital but relatively large delocalization *via* d_{yz}. Simultaneously, this plot restricts a-value as $a = 0.983$–0.988. For β-coefficient calculations we plot product α^2a^2 *vs.* a from g_z-value. Such a plot shows that $\alpha^2a^2 = 0.50(5)$ whereas the plot of β^2 *vs.* α^2a^2 shows that $\beta^2 = 0.93(2)$. Thus, the resulting molecular orbital parameters give the following spin densities on the central ion orbitals: $a^2 = 0.97(3)$, $\alpha^2 = 0.53(1)$, $\beta^2 = 0.93(2)$, ${\gamma_1}^2 \approx 1$ and ${\gamma_2}^2 = 0.55(5)$. The mixing coefficient a value shows a relatively small admixture of $|z^2\rangle$ orbital in the ground state $|x^2 - y^2\rangle$. Thus, a delocalization of spin densities *via* the admixture state is negligible confirming planar structure of the Cu(II) complex. Large delocalization takes place *via* $|x^2 - y^2\rangle$ indicating a strong coordination bonding of Cu(II) by betaine oxygen atom O(2). The ${\gamma_1}^2 \approx 1$ indicates that the delocalization to Br^- ligand *via* out-of plane orbital $|xz\rangle$ is negligible and the Cu–Br bond has mostly ionic character with the two bromine anions ensuring charge compensation for Cu(II). A large spin delocalization appears unexpectedly *via*

$|yz\rangle$ orbital directed towards the betaine O(1) in COO-group. Thus, the main coordination bond is Cu(1)–O(2) while the Cu(1)–O(1) can be considered as a weak coordination bond. It seems to suggest that although betaine acts here as a unidentate ligand, its essentially bidentate character is perceptible as a coupling to the central ion *via* its out-of plane orbital.

4. Conclusion

The molecules in [1-methyl-3-carboxymethyl benzimidazolium betaine]$_2$CuBr$_2$ crystal are stacked with Cu(II) ions forming a chain along the *a*-axis. However, the coupling between neighboring copper ions along the chain is very weak and 1-dimensional magnetic character does not appear. Cu(II) complex has two uncommon properties. The complex is planar with chromophore CuO_2Br_2 (most such complexes have distorted tetrahedral structure) and with unidentate coordination of betaine carboxylate group (in most cases carboxylate group acts as a strong bidentate ligand). Local magnetic properties of Cu(II) complex determined from EPR measurements confirm perfectly planar complex geometry and an analysis of EPR *g*-factors in terms of Molecular Orbital theory shows strong delocalization of the spin density onto ligands in the coordination plane and allow to detect coupling *via* out-of -plane orbital to the more distant oxygen atom of the coordinating betaine.

References

1 Z. Z. Wen, X. L. Wen, S. L. Cai, S. R. Zheng, J. Fan and W. G. Zhang, *CrystEngComm*, 2013, **15**, 5359.
2 O. H. Al-Obaidi, *Bioinorg. Chem. Appl.*, 2012, 601879.
3 B. Das and J. B. Baruah, *Polyhedron*, 2012, **31**, 361.
4 M. Aljahdali, *Spectrochim. Acta, Part A*, 2013, **112**, 364.
5 M. A. Iqbal, R. A. Haque, M. B. K. Ahamed, A. M. S. A. Majid and S. S. Al-Rawi, *Med. Chem. Res.*, 2013, **22**, 2455.
6 (*a*) S. Wadud, R. Onodera, M. M. Or-Rashid and S. Oshiro, *Curr. Microbiol.*, 2001, **42**, 12; (*b*) J. Pacheco-Torres, E. Perez-Mayoral, E. Soriano and P. Lopez-Larrubia, *Synthesis*, 2006, 3859; (*c*) R. S. Keri, A. Hiremathad, S. Budagumpi and B. M. Nagaraja, *Chem. Biol. Drug Des.*, 2015, **86**, 19.
7 (*a*) E. Rozners, R. Smicius and Ch. Uchiyama, *Chem. Commun.*, 2005, 5778; (*b*) A. D. Saleh and P. S. Miller, *Nucleosides, Nucleotides Nucleic Acids*, 2011, **30**, 235.
8 C. Lamberth, R. Dumeunier, S. Trah, S. Wendeborn, J. Godwin, P. Schneiter and A. Corran, *Bioorg. Med. Chem.*, 2013, **21**, 127.
9 Y. T. Wang, G. M. Tang, Y. Wu, X. Y. Qin and D. W. Qin, *J. Mol. Struct.*, 2007, **831**, 61.
10 H. X. Chen, X. P. Xu, Q. F. Xu, Y. Zhang, H. Li, N. J. Li, B. Wu and J. M. Lu, *Polyhedron*, 2012, **41**, 77.
11 H. Yao, Y. Q. Xie, X. Q. Yao, Y. X. Yang and Y. M. Zhang, *Acta Crystallogr., Sect. E: Struct. Rep. Online*, 2013, **69**, o546.
12 J. Miao, Y. Nie, H. W. Chen, J. T. Lia and D. Wang, *Acta Crystallogr., Sect. E: Struct. Rep. Online*, 2009, **65**, o2005.
13 S. S. Massoud, A. A. Galloa, M. J. Dartez, J. G. Gautreaux, R. Vicente, J. H. Albering and F. A. Mautner, *Inorg. Chem. Commun.*, 2014, **43**, 35.
14 P. C. A. Bruijnincx, M. Lutz, A. L. Spek, E. E. van Faassen, B. M. Weckhuysen, G. van Koten and R. J. M. Klein Gebbink, *Eur. J. Inorg. Chem.*, 2005, 779.
15 W. C. Yang, J. Li, J. Li, Q. Chen and G. F. Yang, *Bioorg. Med. Chem. Lett.*, 2012, **22**, 1455.
16 M. Danaher, H. De Ruyck, S. R. H. Crooks, G. Dowling and M. O'Keeffe, *J. Chromatogr. B: Anal. Technol. Biomed. Life Sci.*, 2007, **845**, 1.
17 J. Vališek, T. Davidek, J. Davidek, P. Traška, F. Kvasnička and K. Velcová, *J. Food Sci.*, 1989, **54**, 1544.
18 B. Kozlevcar and P. Segedin, *Croat. Chem. Acta*, 2008, **81**, 369.
19 S. K. Chawla, M. Arora, K. Nattinen, K. Rissanen and J. V. Yakhmi, *Polyhedron*, 2004, **23**, 3007.
20 B. Jasiewicz, B. Warzajtis and U. Rychlewska, *Polyhedron*, 2011, **30**, 1703.
21 X. Meng, L. Liu, H. Zhang, Y. Luoa and C. Liu, *Dalton Trans.*, 2011, **40**, 12846.
22 E. K. Efthimiadou, N. Katsaros, A. Karaliota and G. Psomas, *Inorg. Chim. Acta*, 2007, **360**, 4093.
23 M. Błaszak, E. Jankowska and T. Kowalik-Jankowska, *Polyhedron*, 2014, **68**, 379.
24 M. Kuczer, M. Pietruszka and T. Kowalik-Jankowska, *J. Inorg. Biochem.*, 2012, **111**, 40.
25 R. Buchtík, Z. Trávníček and J. Vančo, *J. Inorg. Biochem.*, 2012, **116**, 163.
26 A. Terenzi, L. Tomasello, A. Spinello, G. Bruno, C. Giordano and G. Barone, *J. Inorg. Biochem.*, 2012, **117**, 103.
27 E. Jankowska, M. Błaszak and T. Kowalik-Jankowska, *J. Inorg. Biochem.*, 2013, **121**, 1.
28 C. Spoerlein, K. Mahal, H. Schmidt and R. Schober, *J. Inorg. Biochem.*, 2013, **127**, 107.
29 G. I. Grasso, G. Arena, F. Bellia, E. Rizzarelli and G. Vecchio, *J. Inorg. Biochem.*, 2014, **131**, 56.
30 D. D. Wu and T. C. W. Mak, *J. Chem. Crystallogr.*, 1996, **26**, 471.
31 L. Diehl, J. Schreuer, E. Haussuhl, B. Winkler, K. Removic-Langer, B. Wolf, M. Lang and V. Milman, *J. Phys.: Condens. Matter*, 2006, **18**, 11067.
32 Y. Li, J. P. Zou, W. Q. Zou, F. K. Zheng, G. C. Guo, C. Z. Lu and J. S. Huang, *Inorg. Chem. Commun.*, 2007, **10**, 1026.
33 X. M. Chen and T. C. W. Mak, *Struct. Chem.*, 1993, **4**, 247.
34 J. Schreuer, L. Wiehl, J. Biehler and P. Hofmann, *Z. Kristallogr.*, 2006, **221**, 529.
35 W. B. Xiang, H. J. Xin, Z. X. Chun, H. Y. Fei and H. H. Wen, *J. Heterocycl. Chem.*, 2000, **37**, 1533.
36 S. Takahashi and H. Kano, *Chem. Pharm. Bull.*, 1968, **16**, 527.
37 *Xcalibur CCD System, CrysAlisPro Software System, Version 1.171.36*, Oxford Diffraction Ltd, Wrocław, Poland, 2012.
38 G. M. Sheldrick, *Acta Crystallogr., Sect. A: Found. Crystallogr.*, 2008, **64**, 112.
39 C. K. Johnson, ORTEP-II, Report ORNL-5138, Oak Ridge National Laboratory, Tennessee, USA, 1976.

40 *Stereochemical Workstation Operation Manual, Release 3.4*, Siemens Analytical X-ray Instruments INC. Madison, 1989.
41 A. Katrusiak, *J. Mol. Graphics Modell.*, 2001, **19**, 362.
42 A. Bondi, *J. Phys. Chem.*, 1964, **68**, 441.
43 K. Golcuk, A. Altun, S. Guner, M. Kumrel and B. Aktas, *Spectrochim. Acta, Part A*, 2004, **60**, 303.
44 G. B. Deacon and R. J. Philips, *Coord. Chem. Rev.*, 1980, **33**, 227.
45 N. Masayuki, T. Hajime and T. Mitsuo, *J. Phys. Chem.*, 1996, **100**, 19812.
46 B. Jasiewicz, M. Hoffmann, A. Gąsowska, R. Jastrząb and K. Malczewska-Jaskóła, *Acta Chim. Slov.*, 2014, **61**, 137.
47 E. di Mauro and W. Saur, *J. Phys.: Condens. Matter*, 1994, **6**, L81.
48 S. K. Hoffmann, J. Goslar and K. Tadyszak, *J. Magn. Reson.*, 2010, **205**, 293.